INFRARED SPECTRA OF LOW-TEMPERATURE STARS*

D. McCammon,† G. Münch, and G. Neugebauer
Mount Wilson and Palomar Observatories
California Institute of Technology, Carnegie Institution of Washington
Received August 5, 1966

ABSTRACT

Spectra of stars of types M, N(R), and S, as well as of NML objects in Cygnus and Taurus, are presented in the regions λλ1 5–1.8 μ and λλ1 9–2 5 μ. In M stars the absorption due to stellar H_2O is apparent from the wings of the bands at λ1.4, λ1.9, and λ2.7 μ Stars of N and S types show weaker H_2O absorption. The $\Delta v = 2$ and $\Delta v = 3$ vibration-rotation band sequences of CO appear well marked in all stars, being somewhat weaker in the M types than in other stars. The late N stars Y CVn and U Hyd show a sharp discontinuity or band head at λ1.76 μ not present in other stars. The entire spectra of Y CVn and U Hyd shortward of this discontinuity appears veiled, the $\Delta v = 3$ CO band sequence being conspicuously weak. The spectra of the NML objects in Cygnus and Taurus have spectral characteristics resembling the carbon more than the M stars.

I. INTRODUCTION

The discovery of stars with extremely low color temperatures by the California Institute of Technology infrared sky survey (Neugebauer, Martz, and Leighton 1965) has raised questions concerning the nature of their atmospheres. Since a large fraction of the energy radiated by these sources is in the infrared, their spectra in this region provide an observational approach to the study of this problem.

Stellar spectra at wavelengths between 1.2 and 2.5 μ have been obtained by Boyce and Sinton (1964), Sinton (1962, 1966), Kuiper (1962, 1963, 1964), Moroz (1966), and Mertz and Coleman (1966) with ground-based telescopes at resolutions on the order of 100. The Stratoscope II observations (Woolf, Schwarzschild, and Rose 1964) have also provided infrared stellar spectra under somewhat lower resolution, but with less telluric absorption. Observations in the regions λλ1.5–1.8 and λλ2.0–2.5 μ appear to be most profitable, as they are relatively free of atmospheric absorption and also contain important spectral features of abundant molecules such as H_2O and CO.

In order to establish the relationship of the extremely red objects to known stars in the spectral sequence, a number of representative M, N, and S stars have been observed to complement measurements of the extremely red sources. To date only two of the latter sources have been observed, but the results obtained so far for the standard stars appear to be of sufficient interest to justify publication of a preliminary description of the spectra.

II. INSTRUMENTATION

The data were obtained with a 0.5-m-focal-length Ebert-Fastie spectrometer originally built for rocket flights. To adapt it for telescopic observations in the PbS infrared range, a 300 groove/mm grating has been installed, providing a dispersion of 31 Å/mm in the second order at λ1.6 μ and 65 Å/mm in the first order at λ2.2 μ. The desired spectral order is isolated with interference filters. The original entrance slit has been replaced by a mirrored plate containing matched pairs of circular apertures of 0.5, 1.0, 1.5, and 2.0 mm diameter, any one of which can be selected to suit resolution and seeing requirements. Guiding is accomplished by viewing the light reflected from this plate through a small telescope. A 5 c/s mirrored chopper located immediately behind the

* Supported in part by National Aeronautics and Space Administration grant NsG-426.

† Presently at the University of Wisconsin.

entrance apertures alternately admits an f/16 beam of radiation from the star and a similar beam from a nearby area of the sky to the spectrometer. The radiation of that beam not entering the spectrometer during a given half of the chopping cycle is reflected to a wide-band ($\lambda\lambda$1.2–2.5 μ) monitor detector.

Liquid-nitrogen-cooled PbS cells with f/1 field lenses are used to detect both the dispersed (signal) radiation and the monitor radiation. The noise-equivalent power of the $\frac{1}{2} \times \frac{1}{2}$ mm cell and 8-mm Si field lens combination used in the signal channel is about 5×10^{-14} watts at 2.2 μ. Signals from both channels are synchronously demodulated and recorded on a single strip chart.

Although the entrance slits used are larger than the apparent stellar disk, seeing fluctuations and imperfections in guiding produce unavoidable variations in the amount of radiation entering the spectrometer. Spurious features arising from these variations are largely eliminated by dividing the signal channel amplitude by the amplitude of the monitor channel output at the corresponding time, thus normalizing the spectrum to constant total energy input.

The wavelength dependence of the response of the spectrometer-detector system has been determined in the laboratory by scanning the radiation of a standard black body. The transmission curves obtained for the two spectral regions of interest are given in Figures 1 and 2, but they have not been incorporated in the stellar spectra presented

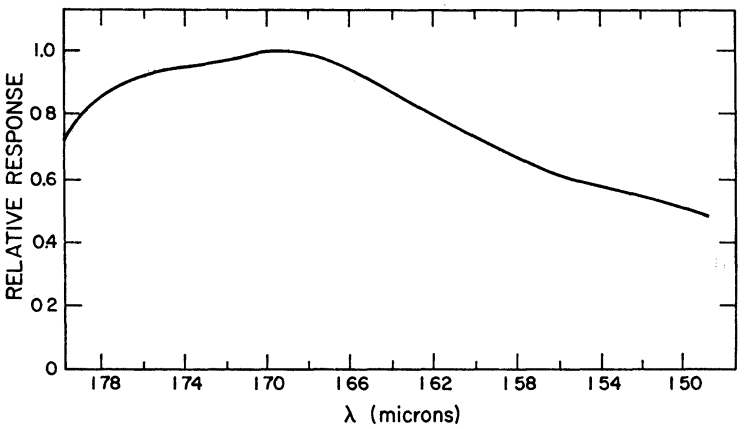

FIG. 1.—Spectrometer system response, $\lambda\lambda$1.5–1.8 μ

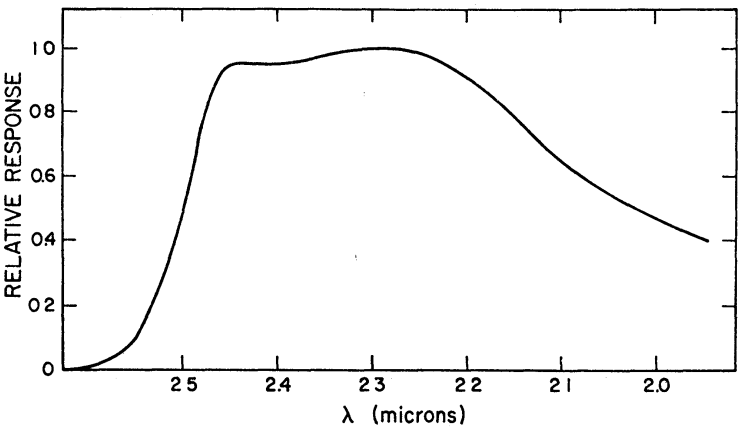

FIG. 2.—Spectrometer system response, $\lambda\lambda$2.0–2.6 μ

here. These curves do not take into account atmospheric attenuation or possible non-gray reflection losses at the telescope mirrors.

III. OBSERVATIONS

Spectra in regions λλ1.5–1.8 and λλ1.9–2.5 μ have been obtained with the spectrometer at the Cassegrain foci of the 24, 60, and 100-inch Mount Wilson reflectors and also at the east arm of the 200-inch Hale telescope at Mount Palomar between July, 1965, and April, 1966. From these observations spectra of twelve stars have been selected for this paper and are given in Figures 3–8. Table 1 lists the observational details associated with each spectrum.

Exit slit widths for the spectra were chosen to obtain the maximum resolution in a reasonable length of time while generally maintaining a signal-to-noise ratio of about 50. Although all spectra in this paper are single scans, each was repeated at least once. An example of the reproducibility generally obtained, as well as of the success of the normalization procedure, is provided in Figure 9, which shows two normalized scans of Y

TABLE 1

JOURNAL OF OBSERVATIONS

Object	Wavelength Range (μ)	Date	Telescope (inches)	Equiv Exit Slit (Å)	RC Time Constant (sec)	Total Scan Time (min)	Scan Rate (Å/sec)	Air Mass
Fig. 3:								
HD 196610	1 5–1 8	Sept. 13, 1965	200	45	1 8	11	5	1 05
R Tri	1 5–1 8	Sept. 13, 1965	200	45	1 8	11	5	1 00
R Cas	1 5–1 8	Sept. 13, 1965	200	45	1 8	11	5	1 05
Mira	1 5–1 8	Sept. 13, 1965	200	45	1 8	11	5	1 26
Fig. 4:								
WZ Cas	1 5–1 8	Sept. 13, 1965	200	45	3 6	11	5	1.12
RS Cyg	1 5–1 8	Sept. 13, 1965	200	45	3 6	11	5	1 00
NML Tau	1 5–1 8	Sept. 12, 1965	200	45	1 8	11	5	1 10
Fig. 5:								
χ Cyg.	1 5–1 8	Apr. 5, 1966	200	12	1 8	22	2 5	1.15
U Hyd	1 5–1 8	Apr. 5, 1966	200	12	1 8	22	2 5	1 50
Y CVn	1 5–1 8	Apr. 6, 1966	200	12	1 8	22	2 5	1 02
Fig. 6:								
Moon.	1 9–2 5	Oct. 10, 1965	24	50	1.8	10	10	1 28
HD 196610	1 9–2 5	Sept. 13, 1965	200	95	1.8	10	10	1 09
R Tri	1 9–2 5	Sept. 13, 1965	200	95	1 8	10	10	1 02
R Cas .	1 9–2 5	Sept. 11, 1965	200	95	3 6	10	10	1 05
Mira ...	1 9–2 5	Sept. 13, 1965	200	95	1 8	10	10	1 27
Fig. 7:								
NML Cyg	1 9–2 5	Sept. 23, 1965	100	95	11	40	2 5	1 07
RS Cyg	1 9–2 5	Sept. 13, 1965	200	95	3 6	10	10	1 00
NML Tau	1 9–2 5	Sept. 21, 1965	100	95	3 6	20	5	1 09
WZ Cas	1 9–2 5	Sept. 13, 1965	200	95	3 6	10	10	1 14
Fig. 8:								
α Ori .	1 9–2 5	Sept. 20, 1965	60	25	1 8	20	5	1 41
χ Cyg. .	1 9–2 5	Apr. 5, 1965	200	25	1 8	20	5	1 09
U Hyd	1 9–2 5	Apr. 5, 1966	200	25	1 8	20	5	1 57
Y CVn	1 9–2 5	Apr. 4, 1966	200	25	1 8	10	10	1 03
Fig. 9:								
Y CVn-S1	1 5–1 8	Apr. 6, 1966	200	12	1 8	22	2 5	1 02
Y CVn-S2	1 5–1 8	Apr. 6, 1966	200	12	1 8	22	2 5	1 02
Fig. 10:								
α Lyr	1 5–1 8	Sept. 13, 1965	200	45	1 8	11	5	1 00
Fig 11:								
α Lyr	1 9–2 5	Sept. 11, 1965	200	95	3 6	10	10	1 01

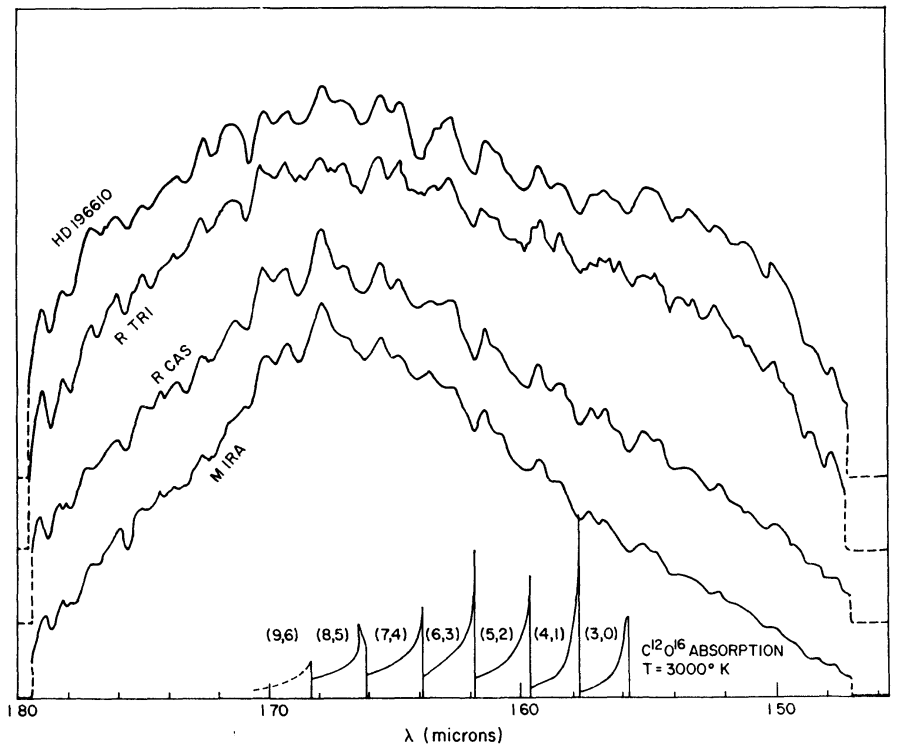

FIG 3.—Spectra of M-type stars in the interval λλ1.5–1.8 μ

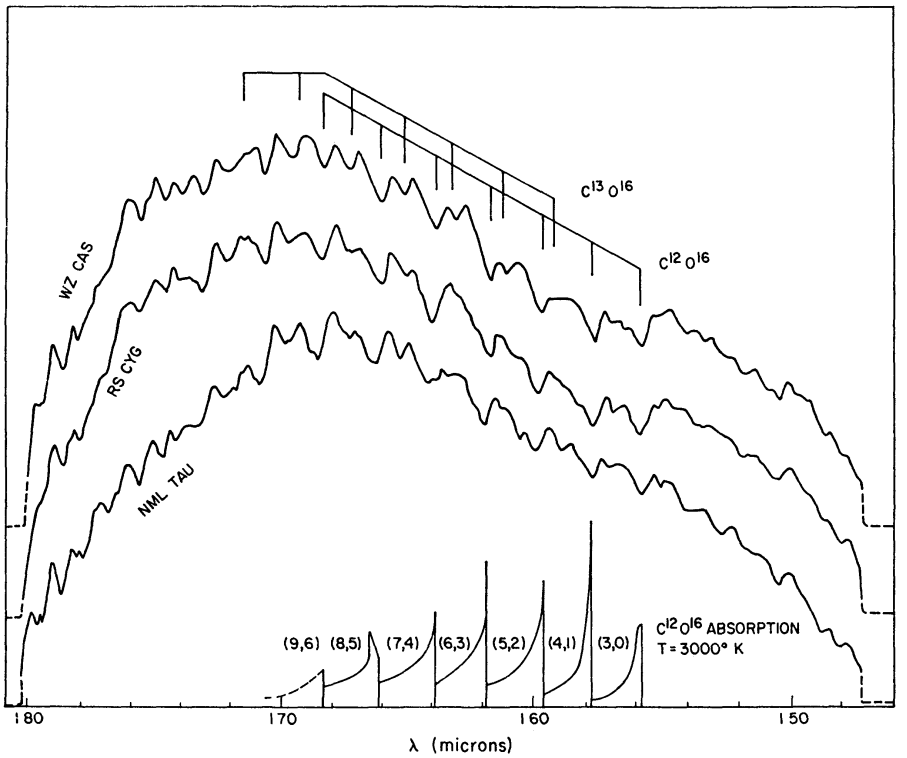

FIG. 4.—Spectra of early carbon stars and of the NML Taurus source, λλ1.5–1.8 μ

Canum Venaticorum along with the monitor channel records used to normalize them. This reproducibility is typical of the spectra shown except that of the NML (Neugebauer, Martz, and Leighton 1965) Cygnus object in Figure 7 which is of lower quality.

An upper limit to the resolution obtainable in a spectral scan is set by the width of the exit slit, which defines the pass band for a fixed point source at the entrance aperture. In practice, accurate guiding is not always possible, and wandering of the stellar image in the entrance slit, which for spectra presented in this paper was 2 mm, may degrade the resolution. For the brighter stars the scanning rates were such that the resolution approached the limit set by the exit slit, whose width is given in the fifth column of

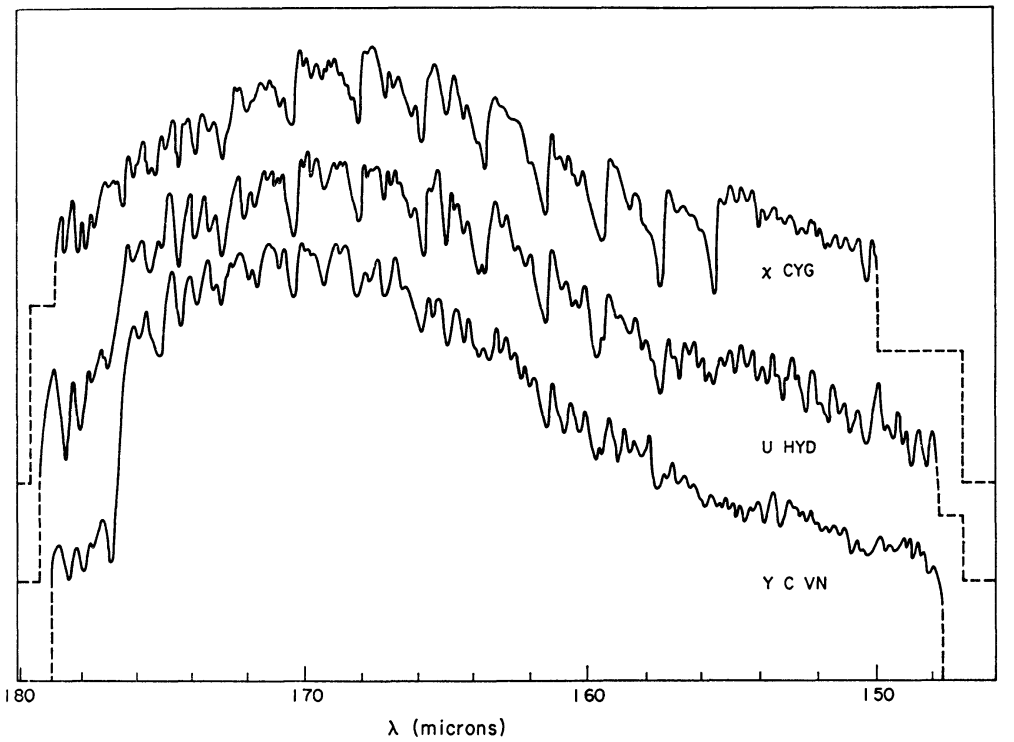

FIG. 5 —Spectra of late carbon stars and χ Cygni, λλ1 5–1.8 μ

Table 1, although a slight shift of features attributable to a slow drift of the stellar image in the entrance slit was sometimes observed over the length of a scan. In the NML Cygnus object, which cannot be observed visually, poorer guiding and slower scanning rates caused the resolution to be determined largely by the 2-mm entrance aperture.

Wavelength calibrations of the spectrometer were done in the laboratory by using emission lines of helium, argon, and mercury. The relative wavelength scale was found to be very stable over long periods of time, but slight shifts of the entire scale have been noted, making it necessary to identify some feature in each spectrum to establish a reference wavelength.

Spectra of α Lyrae, α Canis Majoris, and the Moon have been obtained in order to determine the influence of the terrestrial atmosphere. The features arising from atmospheric absorption are indicated in the spectrum of α Lyrae shown in Figures 10 and 11. No attempt has been made to subtract the telluric features from the spectra given in this paper.

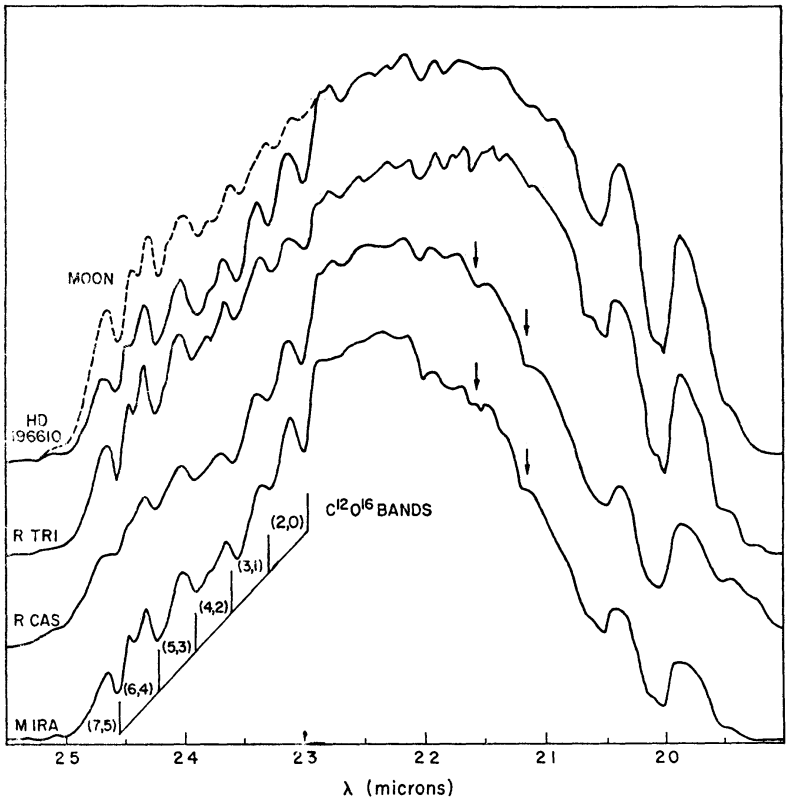

FIG 6.—Spectra of M-type stars in the interval λλ1 9–2 5 μ

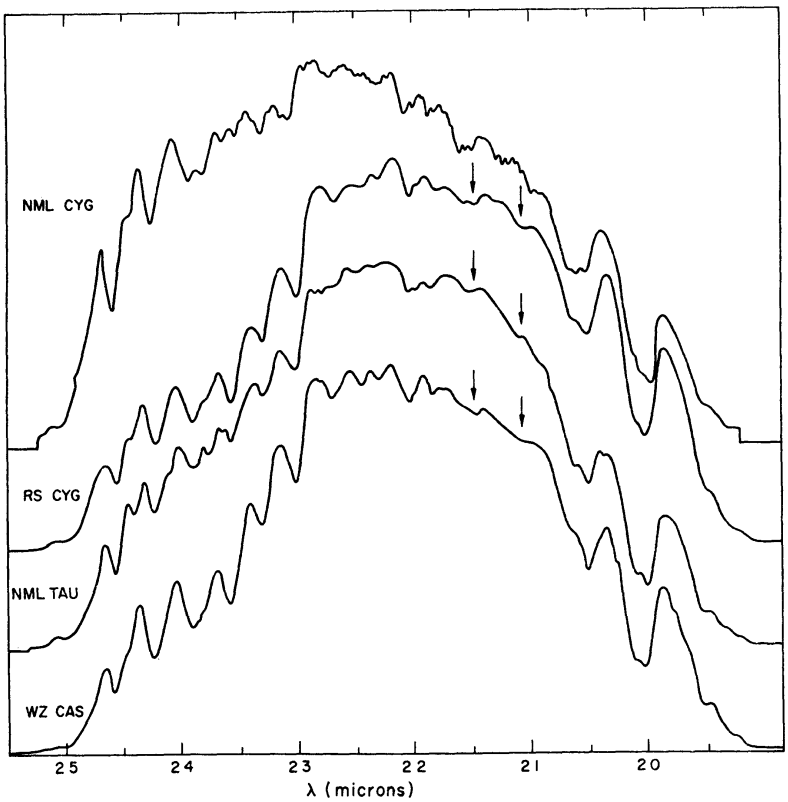

FIG. 7.—Spectra of early carbon stars and of the NML Cygnus and Taurus sources, λλ1 9–2.5 μ

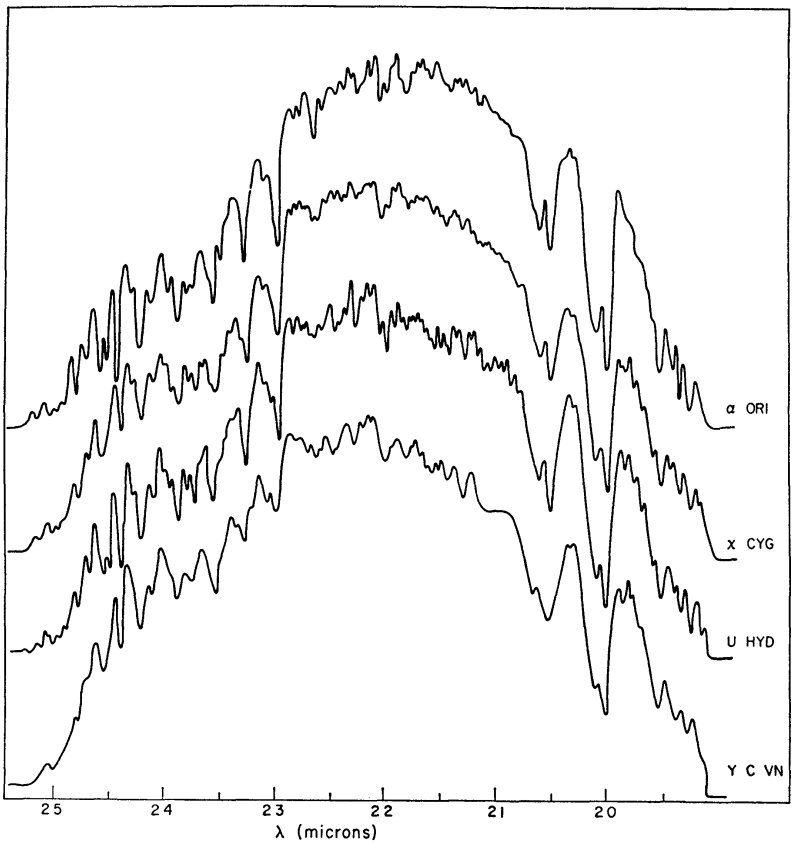

FIG. 8.—Spectra of late carbon stars, α Orionis, and χ Cygni, $\lambda\lambda 1.9$–$2.5\ \mu$

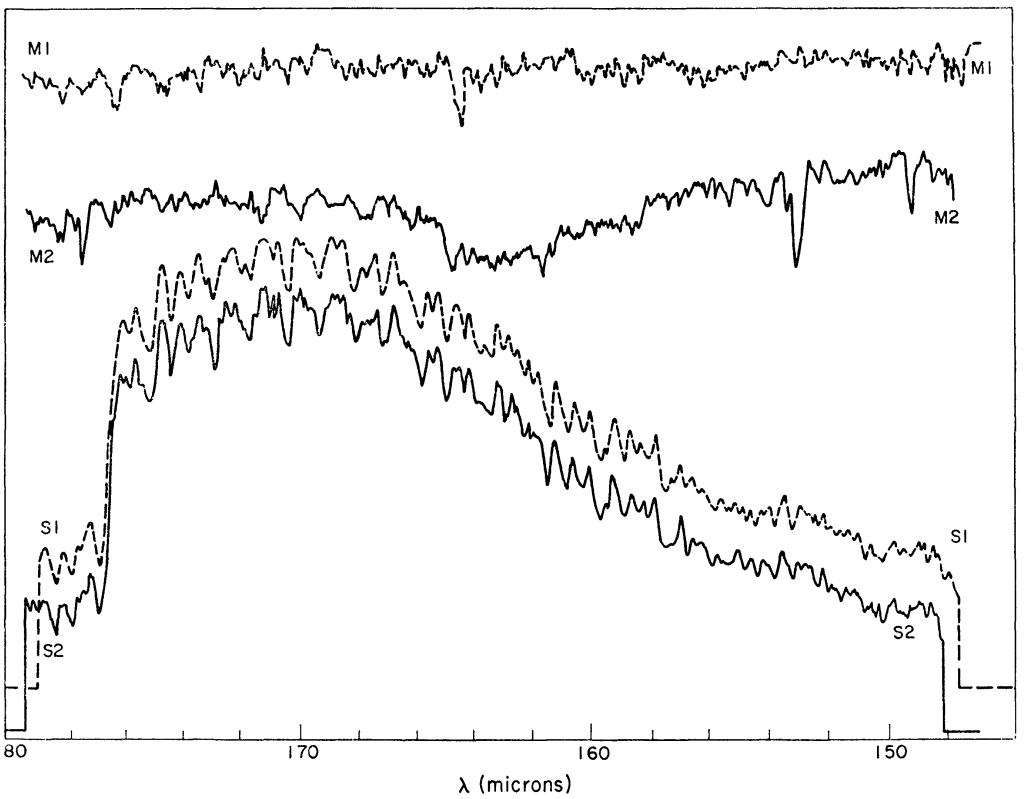

FIG. 9.—Two normalized scans of Y Canum Venaticorum (S1, S2) and their respective monitor records (M1, M2).

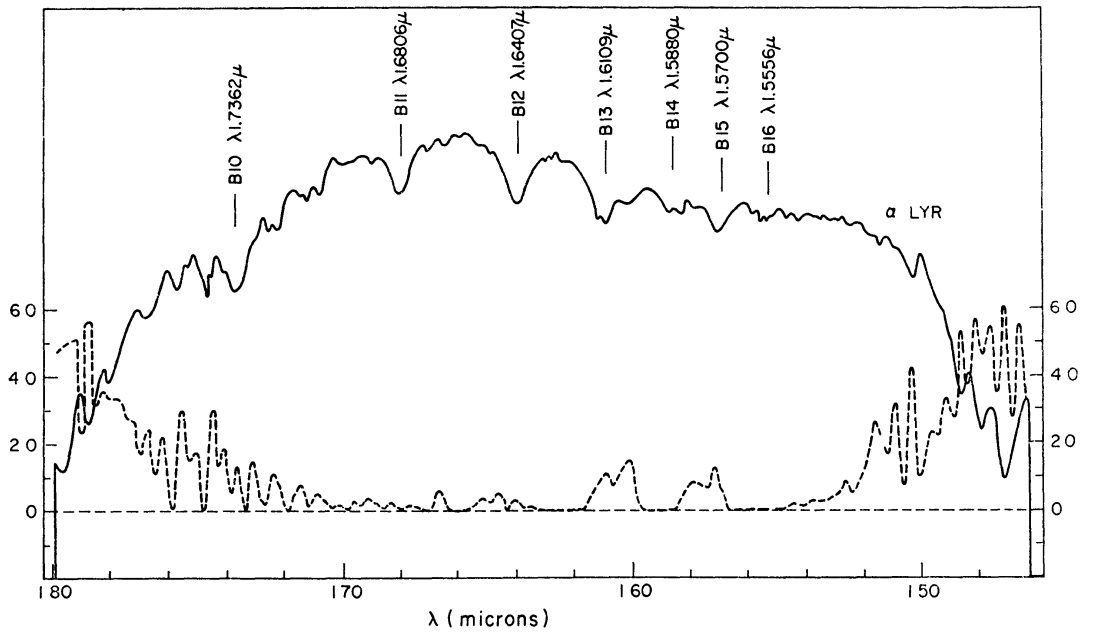

FIG. 10.—α Lyrae, λλ1.5–1 8 μ. Lines due to the Brackett series of atomic hydrogen are indicated. The absorption coefficient of the terrestrial atmosphere is plotted at the bottom of the figure.

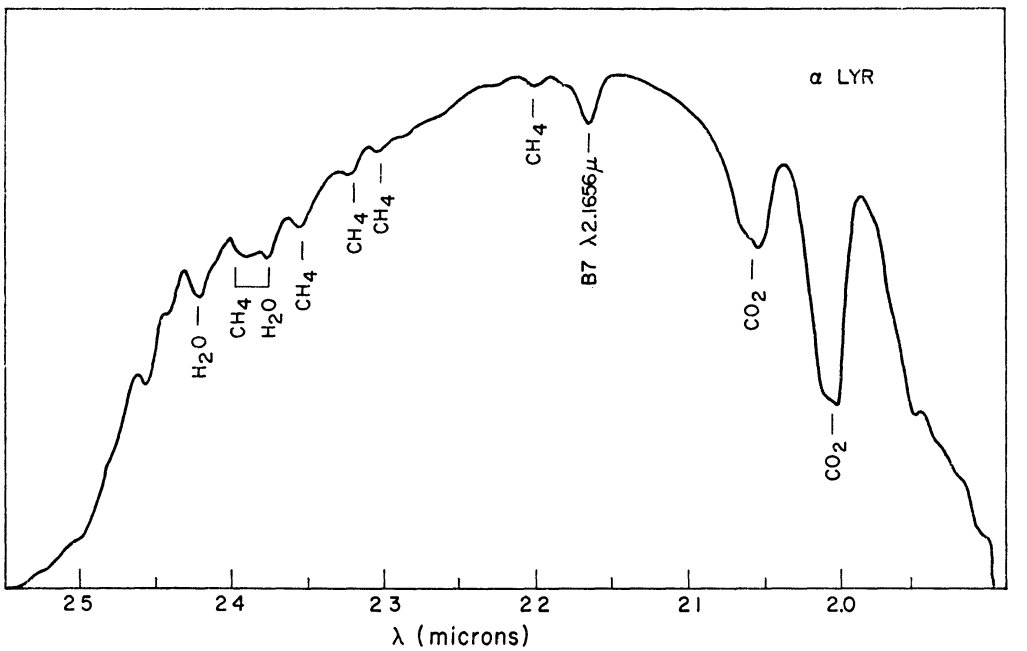

FIG. 11.—α Lyrae, λλ1.9–2.5 μ. Features due to terrestrial atmospheric absorption are indicated

IV. DESCRIPTION OF THE SPECTRA

a) Region λλ1.5–1.8 μ

1. *M stars.*—Spectra of the M-type stars in the region λλ1.5–1.8 μ are shown in Figure 3 in a sequence of decreasing temperature from top to bottom. The most conspicuous feature of these spectra is the extended absorption of the λ1.4- and λ1.9-μ bands of stellar H_2O, which for lower temperatures has a deeper minimum around λ1.68 μ (Ferriso, Ludwig, and Thomson 1966). Thus the apparent maxima of the spectra around λ1.68 μ become more pronounced. The observers of Stratoscope II (Woolf *et al.* 1964) have suggested that the peak at λ1.68 μ may be caused to some extent by the minimum value taken by the continuous absorption coefficient of H^- around this wavelength.

A series of prominent band heads starting at λ1.56 μ is readily identified with the R-heads of the vibration-rotation bands of the third overtone of CO. The absorption coefficient of the CO molecule at a temperature of 3000° K, averaged over intervals of 10 Å, is plotted at the bottom of Figure 3. The correspondence between the wavelengths of the stellar features and the calculated CO absorption from the (3,0) band up to the (9,6) band at λ1.70 μ can be seen despite the overlap that exists among the higher bands in this sequence. Little can be inferred from either the apparent relative intensities or the temperature dependence of these stellar features without more detailed study, since variations in the slope of the underlying stellar H_2O absorption with temperature and occasional coincidences with telluric or additional stellar features probably mask the actual band strengths. The 3000° K temperature was chosen only for convenience in plotting the CO absorption coefficient.

2. *N(R) and S stars.*—The spectra of the carbon stars WZ Cassiopeiae and RS Cygni shown in Figure 4 have a shape quite different from that of the M-type spectra. The absorption of the λ1.4- and λ1.9-μ H_2O bands is weaker, and consequently the intensity maximum at λ1.68 μ is more rounded than in the cooler M types. The onset of the CO absorption at λ 1.56 μ, on the other hand, is more conspicuous; the higher bands of the $\Delta v = 3$ sequence appear more clearly defined than in the M stars and seem to produce an appreciable depression in the apparent continuum. Again, this is probably due to the weakness of the H_2O absorption in this spectral region.

In the star WZ Cas, known to be rich in C^{13} from the intensities of the isotopic Swann bands, features occur at wavelengths corresponding to the band heads of the $C^{13}O^{16}$ $\Delta v = 3$ band sequence which do not seem to be apparent in other stars.

The spectra of the later N-type stars Y Canum Venaticorum and U Hydrae are given in Figure 5 with a resolution about twice that typical of Figures 3 and 4. The most remarkable feature of these spectra is the sharp discontinuity at λ1.76 μ, which is not shown by any of the other carbon stars observed. The existence of a sudden decrease in intensity shortward of about λ4000 Å in the spectrum of Y CVn and other N-type stars has been known for many years (Shajn and Struve 1947) and has been attributed to the absorption produced by C_3. The spectrum shortward of λ1.76 μ in Y CVn and U Hyd also shows marked differences from other stars. For comparison purposes a spectrum of χ Cygni with a comparable resolution is included in Figure 5. The weakness of the $\Delta v = 3$ sequence of CO bands in the late N-type stars is quite obvious, and, in fact, the (3,0) band of CO appears completely obliterated in Y CVn. Since, as seen in Figure 8, the $\Delta v = 2$ band sequence of CO is not weakened in these same late N-type stars, and since there are no indications of strong H_2O absorption, another source of absorption must be affecting the entire spectrum in this region. On the basis of the observed spectral characteristics of the late N-type stars in the photographic region, it would be logical to hypothesize that this absorption is produced by a polyatomic carbon compound, such as C_3 or SiC_2.

The spectrum of the S star S Ursa Majoris, not reproduced in this paper, closely re-

sembles that of χ Cyg, which is an intermediate object between S- and M-type stars. The $\Delta v = 3$ band sequence of CO appears as strong in χ Cyg as in the early carbon stars. The general shape of these spectra suggests the absence of the H_2O absorption apparent in the spectrum of Mira. This conclusion is in agreement with the findings of Wing, Spinrad, and Kuhi (1967) in the photographic region.

b) Region λλ1.9–2.5 μ

1. *M stars.*—The appearance of the M-type stars in the λλ1.9–2.5-μ region (Fig. 6) is dominated by the H_2O absorption band at λ1.9 μ, the wings of which extend further into the red as the temperature decreases. This absorption, combined with the shift of the energy peak to the red and the absorption of the $\Delta v = 2$ rotation-vibration bands of CO beyond 2.3 μ, produces a sharper apparent maximum at around λ2.25 μ in the cooler stars. The head of the (2,0) band of CO produces a discontinuity in the spectrum at λ 2.30 μ. The spectral region covered by the $\Delta v = 2$ sequence of CO bands is heavily affected by telluric absorption due to CH_4 and H_2O, as is seen in the spectrum of the Moon which has been superimposed on that of HD 196610 in Figure 6. Nevertheless, these CO bands can be distinguished as has been reported by Boyce and Sinton (1964). The spectra of the cooler stars, Mira and R Cas, show two distinct shallow absorption features at λ2.13 and λ2.16 μ which have not been identified. Sinton (1966) has observed similar features and attributed them to CH.

2. *N(R) and S stars.*—As in the λλ1.5–1.8-μ region, the carbon stars shown in Figure 7 are affected less than the M stars by stellar H_2O absorption and, as a consequence, their spectra are flatter. The $\Delta v = 2$ band sequence of CO is also prominent in the carbon stars, but it has a somewhat different appearance than in the M stars. In particular, the CO bands around λ2.4 μ are more distinct in the carbon than in the M stars; this probably is also an effect of the decrease in the underlying H_2O absorption. The spectrum of WZ Cas reproduced in Figure 7 does not show any feature that can be identified with certainty with $C^{13}O^{16}$, possibly due to the lower resolution of these spectra. The unidentified features at λ2.13 and λ2.16 μ noticed in the M stars are also present in WZ Cas and RS Cygni.

The spectra of two later N-type stars and of χ Cygni are shown in Figure 8 at a resolution higher than that in the preceding figures. The spectrum of α Orionis, an M star, has been included for comparison purposes. As previously mentioned, the $\Delta v = 2$ CO bands are not weakened in the late N-type stars as the $\Delta v = 3$ bands were found to be. The unidentified features at λ2.11 and λ2.16 μ seem to be stronger in the spectrum of the late N types.

c) The NML Stars in Cygnus and Taurus

Since the main infrared spectral characteristics of the observed M-, N-, and S-type stars can be attributed to absorption bands of H_2O and CO, it is of interest to analyze the behavior of these features in the spectra of the NML stars in Cygnus and Taurus. The spectra of these objects in the λλ1.9–2.5-μ region appear together with those of WZ Cas and RS Cyg in Figure 7. The spectrum of the Cygnus object clearly is unique because of its high average energy around λ2.4 μ, a feature which might actually be a temperature effect or might be produced by heavy interstellar reddening. The flatness of the spectrum in the λλ2.1–2.2-μ region indicates that the H_2O absorption due to the λ1.9-μ band is weak relative to that in the Mira-type variables. The weakness of the H_2O absorption is also indicated by the definition of the (7,5) and (6,4) CO bands. Thus, with regard to the H_2O absorption, the Cygnus object resembles a carbon star more than an M-type star. The spectrum of the Taurus source shows similar, although less pronounced, characteristics.

Because of the faintness of the Cygnus object in the λλ1.5–1.8-μ region, no spectrum of this source with a quality comparable to the other spectra in this paper has been ob-

tained. However, the spectra available do not show any features strikingly different from those appearing in other stars. In particular, there is no sign of the unidentified absorption detected in the late N-type stars. The spectrum of the Taurus object in the λλ1.5–1.8-μ region appears in Figure 4, where its similarity to that of the carbon stars can be noticed. When the spectrum of the Taurus object is made to agree with that of an M star such as R Cas in the region λλ1.6–1.7 μ, the spectrum of the Taurus object is somewhat higher than that of the M type around λ1.55 and λ1.75 μ. The weakness of the H_2O extended absorption is thus also apparent in this region. The low H_2O content of the Cygnus and Taurus objects and their consequent similarity to the carbon stars has been pointed out by Wing *et al.* (1967) on the basis of the appearance of the H_2O band at λ9400 Å.

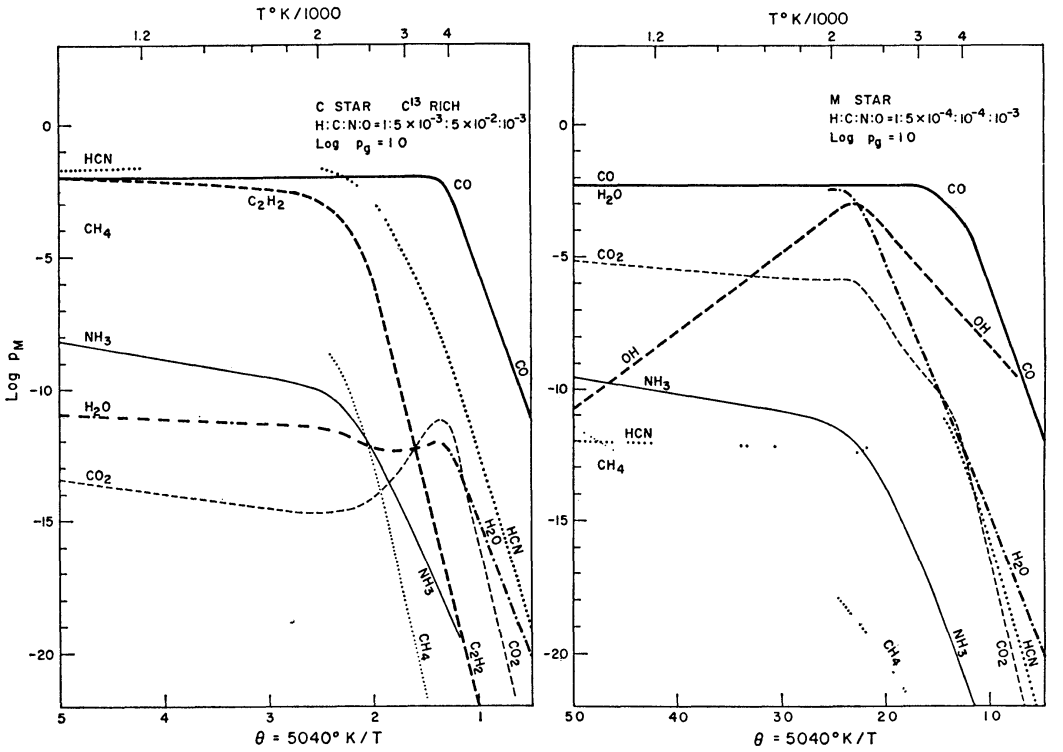

FIG. 12.—Calculated molecular dissociation equilibria (after Tsuji 1964)

V. CONCLUSIONS

The observations of low-temperature stars presented here have shown that their infrared spectral characteristics are primarily determined by the absorption due to H_2O. In the cooler M-type stars the H_2O absorption is very strong relative to that observed in the N- and S-type stars. The NML objects in Taurus and Cygnus in this respect resemble the carbon rather than the M-type stars.

The behavior of the H_2O absorption is readily understood in terms of variations in the C:O abundance ratio. In order to consider qualitatively the general features of stellar spectra in the infrared, the dissociation calculations of Tsuji (1964) for abundance ratios H:C:O:N corresponding to M stars and to carbon stars are shown in Figure 12. The concentration of CO is seen to be about the same in both cases, but that of H_2O is drastically reduced in carbon stars.

The large concentration of some molecular species predicted at these temperatures is also interesting. In the M stars, for example, OH should be an abundant constituent. It

has not been observed, however, even though the $\Delta v = 2$ band sequence of OH lies in the region $\lambda\lambda 1.5$–$1.8\ \mu$ (Chamberlain 1961). The (9,7) band has an origin at $\lambda 2.15\ \mu$, near the unidentified features noted above, but the very open structure of the OH bands and the fact that the unidentified features appear in carbon stars as well as in M-type stars rules out their identification with OH. Evidently, an attempt to detect OH will require higher resolving power than the one used here.

The large concentration of HCN and C_2H_2 predicted in carbon stars is also remarkable. The former molecule has bands at $\lambda 1.53$ and $\lambda 2.01\ \mu$, while the latter is known to have bands at $\lambda 1.54$, $\lambda 2.14$, and $\lambda 2.42\ \mu$. In the spectra available no features can be ascribed to either of these two molecules.

The observation of strong absorption features, presumably due to polyatomic molecules, in the spectra of late N-type stars brings up the question of why even cooler stars, such as the Cygnus object, do not also show very strong absorption features not identifiable with diatomic molecules. As Tsuji (1964) has pointed out, however, below 2200° K the partial pressure of free carbon exceeds the saturated vapor pressure of graphite, and thus it is possible that graphite particles can precipitate, producing a decrease in the concentration of other polyatomic carbon compounds.

A quantitative understanding of the energy curves of the low-temperature stars in the infrared and of their main spectral absorption features will have to be based on calculated model stellar atmospheres. We propose to return to this aspect of the problem at a later date.

The spectrometer has been loaned to us by the Space Sciences Division of the Jet Propulsion Laboratory. We thank all the members of the California Institute of Technology infrared astronomy group, but especially E. Becklin and C. Spencer, for their efforts supporting this work. We are indebted to Dr. Aert Schadee for calculating the absorption coefficient of the rotation-vibration bands of CO and to M. Katz for her help in reducing the data. We thank Dr. William S. Benedict for a helpful discussion.

REFERENCES

Boyce, P. B., and Sinton, W. M. 1964, *Sky and Telescope*, **29**, 78.
Chamberlain, J. W. 1961, *Physics of the Aurora and Airglow* (New York: Academic Press), p. 368.
Ferriso, C. C., Ludwig, C. B., and Thomson, A. L. 1966, *J. Quant. Spectrosc. Rad. Transfer*, **6**, 241.
Kuiper, G. P. 1962, *Com Lunar and Planet. Lab.*, **1**, 179.
———. 1963, *ibid.*, **2**, 17.
———. 1964, *Mém. Soc. R. Sci. Liège*, Ser. 5, **9**, 365 (12th Int. Astr. Col , Liège, 1963).
Mertz, L., and Coleman, I. 1966, *Ap. J.*, **143**, 1000.
Moroz, V. I. 1966, *Astr. Tsirk.* (Sternberg Institute) No. 368, **4**, April 1966.
Neugebauer, G., Martz, D. E., and Leighton, R. B. 1965, *Ap. J.*, **142**, 399.
Shajn, G., and Struve, O. 1947, *Ap. J* , **106**, 86.
Sinton, W. M. 1962, *Appl. Optics*, **1**, 105.
———. 1966, Meeting of Am. Astr. Soc., Hampton, Virginia, March, 1966.
Tsuji, T. 1964, *Ann. Tokyo Astro. Obs.*, **9**, No. 1.
Wing, R. F., Spinrad, H., and Kuhi, L. V. 1967, *Ap. J.*, **147**, 117.
Woolf, N. J., Schwarzschild, M., and Rose, W. K. 1964, *Ap. J.*, **140**, 833.